A Bio-Inspired Approach for Streaming Applications in Wireless Sensor Networks based on the Lotka-Volterra Competition Model

Pavlos Antoniou and Andreas Pitsillides

Department of Computer Science, University of Cyprus, 78 Kallipoleos street, Nicosia, CY-1678, Cyprus.

Abstract

In the new era of Ambient Intelligence, Wireless Sensor Networks (WSNs) are seen to bridge the gap between physical world and the Internet, making a large amount of information accessible anywhere, anytime. Over the last few years, WSNs are being developed towards a large number of multimedia streaming applications, e.g., video surveillance, traffic control systems, health monitoring, and industrial process control. WSNs consist of small sensor devices (nodes) that are capable of working unattended, without centralized control, under dynamically changing conditions. However, these devices face important limitations in terms of energy, memory and computational power. The uncontrolled use of limited resources in conjunction with the unpredictable nature of WSNs in terms of traffic load injection, wireless link capacity fluctuations and topology modifications may lead to congestion. Congestion can cause increased packet loss and delay, as well decrease of network lifetime. This paper proposes a bio-inspired congestion control approach for WSNs streaming applications that necessitate controlled performance with graceful degradation. In the proposed approach, congestion in WSNs is prevented (or at least minimized) by regulating the rate of each traffic flow based on the Lotka-Volterra competition model. Performance evaluations reveal that the proposed approach achieves adaptability to changing traffic loads, scalability and fairness among flows, while providing graceful performance degradation as the offered load increases.

Keywords: Wireless Sensor Networks (WSNs), streaming applications, congestion control (CC), Lotka Volterra (LV) competition model.

1. Introduction

Rapid technological advances and innovations in the area of autonomous systems push the vision of Ambient Intelligence from concept to reality. Networks of autonomous wireless sensor devices offer exciting new possibilities for achieving sensory omnipresence: small, (often) inexpensive, untethered sensor devices can observe and measure various environmental parameters, thereby allowing real-time and fine-grained monitoring of physical spaces around us. Wireless Sensor Networks [1], can be used as platforms for health monitoring, battlefield surveillance, environmental observation, industrial control etc.

Despite the utmost importance of performance control, this issue has not been given adequate attention from the research community. One of the main reasons is that research on WSNs has been heavily influenced by military applications in which dense, large-scale networks of sensors are expected to be deployed in a random manner, primarily with a view to tracking objects.

However, most of the aforementioned critical applications necessitate small-scale networks with planned deployment of sensors close to selected locations/objects of interest in order to achieve controlled performance. The proposed approach is designed on the basis of providing performance control for critical applications in small-scale WSNs.

Typically, WSNs consist of small, cooperative devices (nodes) which may be constrained by computation capability, memory space, communication bandwidth and energy supply. However, with the rapid development of low-cost hardware CMOS cameras and microphones, autonomous sensor devices are becoming capable of ubiquitously retrieving multimedia content such as audio and low-rate video streams from the environment [2]. The unpredictable nature of traffic load injected into the network as well as the uncontrolled use of the scarce network resources (buffer size, wireless channel capacity) are able to provoke *congestion*. Thus, there is an increased need to design novel congestion control strategies possessing emerging properties like self-adaptability, self-organization as well as scalability and fairness, which are vital for dependable WSNs.

The *focal point of this study* is to propose a *scalable and self-adaptive bio-inspired congestion control mechanism* targeting streaming applications in WSNs for delivering enhanced application fidelity at the sink (in terms of packet delivery ratio and delay) under varying network conditions. More specifically, the *main objective is to provide efficient and smooth rate allocation and control while maintaining fairness and friendliness with interfering flows*. Biological processes which are embedded in decentralized, self-organizing and adaptive environments, provide a desirable basis for computing environments that need to exhibit such properties.

Population dynamics has traditionally been the dominant branch of mathematical biology which studies how species populations change in time and space and the processes causing these changes. Information about population dynamics is important for policy making and planning and in our case is used for designing a congestion control policy. This study focuses on the Lotka-Volterra (LV) competition model, and proposes a decentralized approach that regulates the rate of every flow in order to prevent, or at least gracefully minimize congestion whilst aiming to achieve fairness among competing flows. The LV-based congestion control (LVCC) mechanism is targeted for small-scale dependable multimedia WSNs [2] and especially for applications that require continuous stream of data.

This paper investigates the global LV system behavior on the basis of simple interactions among competing species. These interactions are viewed at the microscopic and the macroscopic level. The validity of the analytical results is further investigated by simulating complex scenarios that cannot be formally tested. Performance evaluations have shown that the LVCC approach provides adaptation to dynamic network conditions providing scalability, fairness, and graceful performance degradation among traffic flows when multiple active nodes are involved.

The remainder of this paper is organized as follows. Section 2 deals with the problem of congestion in WSNs while Section 3 discusses related work. Section 4 sheds light on the insights of the LV competition model. Section 5 presents the analogy between WSNs and ecosystems and proposes the LV-based Congestion Control (LVCC) mechanism. Section 6 presents the performance evaluation of LVCC. Section 7 draws the conclusion and future work.

2. Congestion in Multimedia Wireless Sensor Networks

Data streaming applications have intrinsic bandwidth, delay and packet loss requirements. Thus, stream flows being left uncontrolled are likely to cause unpredictable traffic load injection into the network, leading to congestion. Congestion occurs when the traffic load injected

into the network exceeds available capacity at any point of the network. In wireless networks, packet losses can be attributed to either *buffer overflows*, or *collisions in the wireless medium* [3], [4] when more than one nodes are trying to access the channel simultaneously assuming a CSMA-like MAC protocol. Note that competing protocols, such as TDMA-based may resolve the problem of wireless channel collisions. The problem of buffer overflows is considered to be more critical in WSNs than the classical Internet due to buffer size limitations. Even at low traffic rates, buffer overflows can be experienced at some point of the network (usually close to the sink) due to the converging (many-to-one) nature of packets from multiple sending nodes to a single sink node.

Congestion may cause multiple packet losses, low link utilization (throughput reduction), and increase of queueing delays, leading to the deterioration of the offered quality of service (QoS). Increasingly, congestion in WSNs is responsible for energy waste, decrease of network lifetime and even for the decomposition of network topology in multiple components.

Due to their severely constrained nature, WSNs necessitate autonomous, decentralized, fast time scale congestion control strategies which promise immediate, effective and efficient relief from congestion. Decentralized approaches are expected to adopt a hop-by-hop model where all nodes along a network path can be involved in the procedure. Each node should make decisions based only on local information (e.g. buffer load, channel load) since none of them has complete information about the system state. This is a desirable feature as it minimizes the exchange of messages, hence improves both energy and congestion.

3. Related Work

Early studies in the area of WSNs had mainly focused on more fundamental networking problems, e.g. medium access control (MAC), topology, routing, and energy efficiency, and had largely ignored network performance assurances. Lately, with the emergence of mission-critical applications, there has been increased interest in performance control mechanisms [5], so as to avoid congestion caused by the uncontrolled use of the scarce network resources.

Various congestion control (CC) approaches can be found in WSNs literature based on traffic manipulation (e.g. rate adaptation to network changes CODA [3], Fusion [4], IFRC [6], multi-path routing BGR [7], topology control (e.g. clustering formation [8]), and network resource management (e.g. power control, multiple radio interfaces Siphon [9]). Rate control approaches are considered to be the most appropriate when dealing with streaming applications. Rate control is a common technique for alleviating congestion by throttling the injection of traffic in the network. Some of the rate-based CC schemes [3], [6], and [7] are based on traditional methodologies and protocols known from the Internet, for example, the Additive Increase Multiplicative Decrease (AIMD) rate control mechanism. This model is not very effective in WSNs because it provokes a saw-tooth rate behavior which may violate the QoS requirements (e.g. fidelity of a stream). In addition, AIMD-like mechanisms take a long time for data rates to converge in low-rate wireless links, which would cause significant variation in streaming media quality. The proposed mechanism was found to outperform AIMD (see Section 6), providing smooth rate allocation and control while maintaining friendliness among competing flows.

4. The Lotka-Volterra (LV) Competition Model

Often, non linear systems are studied in terms of simple mathematical biology models [10] which aim at modeling natural and biological processes using analytical techniques and tools.

Population dynamics has traditionally been the dominant branch of mathematical biology which studies how populations of species change in time and space as well as the processes that cause these changes. Information about population dynamics is of fundamental importance for policy making and planning.

Population dynamics can be modeled with a simple balance equation that describes how the overall population size of a species changes over time as a result of species interaction with resources, competitors, mutualists and natural enemies. This study adopts similar ideas so as to design congestion avoidance strategies for competing streams of data. The proposed approach is based on *a deterministic competition model which involves interactions among species that are able to coexist, in which the fitness of one species is influenced by the presence of other species that compete for at least one limiting resource*. An in depth investigation and modeling of competitive interactions between organisms provides an initial basis for predicting outcomes.

This study focuses on the Lotka Volterra (LV) competition model [11], [12], which is considered to be one of the most studied mathematical models of population biology.

4.1. The Microscopic Level of System Behavior: Interactions and Rules

The global behavior of a biological system emerges from simple interactions. These interactions can be viewed at different levels: the microscopic level describes the entities involved and their behavior; the macroscopic level describes the (emergent) behavior of the overall system. From the *microscopic level*, the species within an LV-based ecosystem follow a set of rules:

1. The population of each species i grows at a given intrinsic growth rate r_i in the absence of all other competing species.
2. Each species i reproduces proportionally to the population of the same species i, by an intra-specific competition coefficient β_i. The parameter β_i represents the competitive effects among individuals of species i;
3. Each species i reproduces proportionally to the population of species j, by an inter-specific competition coefficient α_{ij}. The parameter α_{ij} represents the competitive effects of species j on growth of species i

If $\alpha_{ij} < \beta_i$, then the competitive effect of species j on population growth of species i is less than that of an individual of species i. The rules can be described in an aggregated form by a set of differential equations.

4.2. The Mathematical Model

The generalized form of an n-species LV system is expressed by a system of ordinary differential equations:

$$\frac{dx_i}{dt} = x_i\left(r_i - \frac{\beta_i r_i}{K_i}x_i - \frac{r_i}{K_i}\left(\sum_{j=1,j\neq i}^{n}\alpha_{ij}x_j\right)\right), \tag{1}$$

for $i = 1, ..., n$, where $x_i(t)$ is the population size of species i at time $t\,(x_i(0) > 0)$. Also K_i is the carrying capacity of species i. K_i the maximum number of individuals of species i that can be sustained by the biotope in the absence of all other species competing for the same resource when $\beta = 1$. Otherwise, the maximum population size of species i can reach K_i/β_i. If only one resource exists and all species (having the same carrying capacity K) compete for it, then K can be seen as the resource's capacity. Next we will build on this model to develop our approach, assuming that the n species have the same characteristics: $r_i = r$, $K_i = K$, $\beta_i = \beta$ and $\alpha_{ij} = \alpha$ for every i, j.

4.3. The Macroscopic Level of System Behavior

In the *macroscopic level*, the system emergent behavior is described in terms of the species populations evolution. According to the analytical study of the LV competition model by [10], the system can be in one of the following states:

1. All species in the system can survive and coexist.
2. At least one species can survive, out-competing the rest and condemning them to extinction.

It is beyond any doubt that these states cannot be intuitively deduced from the microscopic rules.

The system of Eq. 1 cannot be analytically solved, but some information about the behavior of its solutions can be obtained. Instead of trying to solve for $x_1, x_2, ..., x_n$ as functions of t, we can eliminate t and look for the relation between all x_i, for $i = 1, ..., n$. In geometric terms, we study the *phase plane*, the (x,y) plane. The phase plane can be used to predict the outcome of competition over time (emergent system behavior). The dynamic path of this many-commodity ecosystem can be determined on the basis of the trajectories (or orbits) of solutions [1]. Conceptually, the state of such a system is represented by a point (a vector of n components) lying on an n-dimensional trajectory and the movement of this point over the trajectory through time is governed by the system of differential equations.

Unfortunately, most problems that arise in the real world are not linear, and in most cases, nonlinear systems can not be solved - there is typically no method for deriving a solution to the equations. When confronted with a nonlinear differential equation system such as the n-dimensional system of Eq. 1, we usually must be satisfied with an approximate solution. One method to find approximate solutions is *linearization* near a constant solution. The equilibria are constant solutions of the system of differential equations (e.g. Eq. 1) that satisfy the equations $dx_i/dt = 0$, for $i = 1, ..., n,$. Geometrically, an equilibrium is a point in the phase plane that is the orbit of a constant solution. Therefore, it seems more convenient to study the behavior of the system around equilibria (if any) and investigate their stability.

In this study, the 2-species LV competition model is taken into consideration when investigating the stability of equilibria. The system of differential equations is given by:

$$\frac{dx_1}{dt} = f(x_1, x_2) = rx_1\left(1 - \frac{\beta}{K}x_1 - \frac{\alpha}{K}x_2\right), \quad \frac{dx_2}{dt} = g(x_1, x_2) = rx_2\left(1 - \frac{\beta}{K}x_2 - \frac{\alpha}{K}x_1\right). \quad (2)$$

An equilibrium is a solution $\left(x_1^*, x_2^*\right)$ of the pair of equations $dx_1/dt = f(x_1^*, x_2^*) = 0$, $dx_2/dt = g(x_1^*, x_2^*) = 0$. There can be distinguished four possible equilibria: (a) $(0, 0)$, (b) $\left(\frac{K}{\beta}, 0\right)$ with $\frac{K}{\beta} > 0$ and $f(\frac{K}{\beta}, 0) = 0$, (c) $\left(0, \frac{K}{\beta}\right)$ with $\frac{K}{\beta} > 0$ and $g(0, \frac{K}{\beta}) = 0$, and (d) $\left(\frac{K}{\alpha+\beta}, \frac{K}{\alpha+\beta}\right)$ with $\frac{K}{\alpha+\beta} > 0$, $f\left(\frac{K}{\alpha+\beta}, \frac{K}{\alpha+\beta}\right) = 0$ and $g\left(\frac{K}{\alpha+\beta}, \frac{K}{\alpha+\beta}\right) = 0$.

The first equilibrium $(0, 0)$ describes the situation in which no species survive. Both equilibria $\left(\frac{K}{\beta}, 0\right)$ and $\left(0, \frac{K}{\beta}\right)$ describe the situation in which one species survives but the other species loses the struggle for existence and becomes extinct. The last equilibrium describes the coexistence of species. In the presence of n species, there will be n equilibrium points: all species coexist, all species extinct, and $n - 2$ combinations of some species surviving and some vanishing. As from a biological point of view only non-negative population sizes are of interest, we consider only equilibria having non-negative coordinates.

[1] Curves in the plane representing the functional relationship between all x_i, $i = 1, ..., n$, with the time t as parameter.

The behavior of solutions near an equilibrium can be determined by the behavior of solutions of the linearization at the equilibrium. The linearization of the system 2 using Taylor's theorem at the equilibrium $\left(x_1^*, x_2^*\right)$ (neglecting higher order terms) gives the coefficient matrix:

$$M\left(x_1^*, x_2^*\right) = \begin{pmatrix} f_x\left(x_1^*, x_2^*\right) & f_y\left(x_1^*, x_2^*\right) \\ g_x\left(x_1^*, x_2^*\right) & g_y\left(x_1^*, x_2^*\right) \end{pmatrix} = \frac{r}{K}\begin{pmatrix} K - 2\beta x_1^* - \alpha x_2^* & -\alpha x_1^* \\ -\alpha x_2^* & K - 2\beta x_2^* - \alpha x_1^* \end{pmatrix}. \tag{3}$$

which is called the *community matrix* of the system at the equilibrium $\left(x_1^*, x_2^*\right)$. It describes the effect of the size of each species on the growth rate of itself and the other species at equilibrium.

An equilibrium $\left(x_1^*, x_2^*\right)$ is said to be *stable* if every solution $(x_1(t), x_2(t))$ with $(x_1(0), x_2(0))$ sufficiently close to the equilibrium remains close to the equilibrium for all $t \geq 0$. An equilibrium $\left(x_1^*, x_2^*\right)$ is said to be *asymptotically stable* if it is stable and if, in addition, all solutions with $(x_1(0), x_2(0))$ sufficiently close to the equilibrium tend to the equilibrium as $t \to \infty$.

The asymptotic stability or instability of a linear system is determined by the eigenvalues of the matrix M. The sum of the eigenvalues is the *trace* of the matrix M and the product of the eigenvalues is the *determinant* of the matrix M. An equilibrium $\left(x_1^*, x_2^*\right)$ is asymptotically stable if all eigenvalues of the coefficient matrix of the linearization at this equilibrium, M, have negative real part, specifically if:

$$\operatorname{tr} M\left(x_1^*, x_2^*\right) = f_x\left(x_1^*, x_2^*\right) + g_y\left(x_1^*, x_2^*\right) < 0, \tag{4}$$

$$\det C\left(x_1^*, x_2^*\right) = f_x\left(x_1^*, x_2^*\right) g_y\left(x_1^*, x_2^*\right) - f_y\left(x_1^*, x_2^*\right) g_x\left(x_1^*, x_2^*\right) > 0. \tag{5}$$

Based on Eqs. 4 and 5, the stability of the equilibrium points depends on the relationship between α and β. When $\beta > \alpha$, only the equilibrium $\left(\frac{K}{\alpha+\beta}, \frac{K}{\alpha+\beta}\right)$ is asymptotically stable (having positive determinant and negative trace), while the other three equilibria of the system 2, namely $(0,0)$, $\left(\frac{K}{\beta}, 0\right)$ and $\left(0, \frac{K}{\beta}\right)$ are classified as unstable. On the other hand when $\beta < \alpha$, only the equilibria $\left(\frac{K}{\beta}, 0\right)$ and $\left(0, \frac{K}{\beta}\right)$ are asymptotically stable.

Each linearization provides a good approximation to the behavior of system 2 near the corresponding equilibrium point. In addition, the eigenvalues at each equilibrium determine the stability of the equilibrium. However, the local linearizations do not tell us what is happening in the phase plane far from the equilibria. In order to provide a better understanding of the system behavior far from equilibria under different initial conditions *phase portraits*[2] graphs are considered. For each species, there is a straight line on the phase portrait called a zero isocline[3] (or nullcline). Any given point along, for example, species 1's zero isocline represents a combination of populations of the two species where the species 1 population does not increase or decrease. Figure 1 shows the zero isoclines for species 1 (left) and species 2 (right).

Note that the zero isoclines divide each phase portrait into two parts. Below and to the left of the isocline the population size increases because the combined populations of both species are less than the maximum population size of each species (K/β, while above and to the right the population size decreases because the combined populations are greater than the K/β. For the phase portrait of species 1, the isocline intersects the graph on the x-axis when x_1 reaches K/β and no individuals of species 2 are present. The isocline intersects the phase portrait on the y-axis

[2] A phase portrait is a geometric representation of a dynamical system which depicts the system's trajectories, the stable steady states and the unstable steady states in the phase plane [13].

[3] The zero isocline for a species is calculated by setting the growth rate, dx/dt, equal to zero and solving for x.

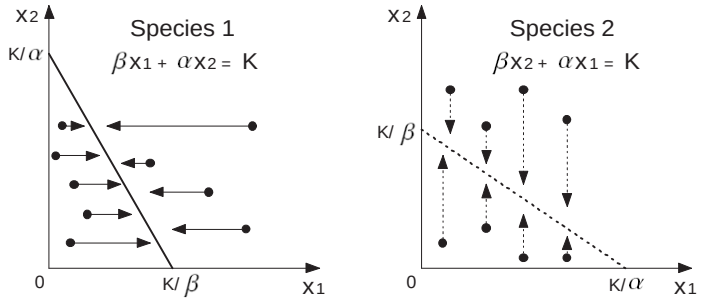

Figure 1: Zero isoclines for (a) species 1 and (b) species 2.

at K/α, when the carrying capacity of species 1 is filled by the equivalent number of individuals of species 2 and no individuals of species 1 are present. The intersections of the isocline for species 2 are essentially the same, but on different axes.

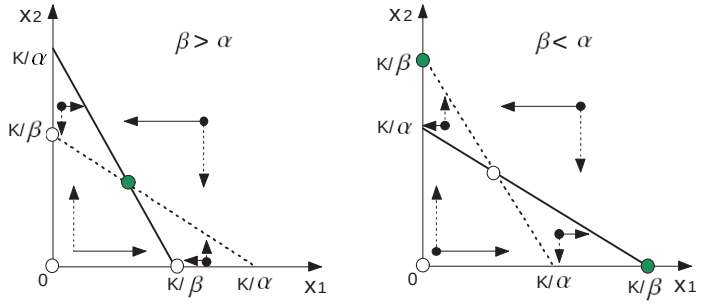

Figure 2: Zero isoclines for species 1 and 2 when (a) $\beta > \alpha$ and (b) $\beta < \alpha$.

The phase portraits of Fig. 2 include both species' isoclines, and illustrate the possible outcomes of interspecific competition depending on where each species' isocline lies in relation to the other. In each phase portrait, the solid line represents the isocline of species 1, and the dashed line represents the isocline of species 2. The arrows indicate the trajectories of species' population sizes for different initial values while converging/diverging to/from systems' equilibria.

Fig. 2(a) shows the isoclines of both species when $\beta > \alpha$. It can be observed that regardless of the initial values of population sizes, all trajectories head toward the intersection of isoclines. More specifically, below and above the two isoclines both populations increase and decrease respectively. Also, when the species populations are between the isoclines their trajectories always are directed to the intersection point. The coordinates of the intersection point are $\left(\frac{K}{\alpha+\beta}, \frac{K}{\alpha+\beta}\right)$ and correspond to the equilibrium point which was analytically found to be stable when $\beta > \alpha$. Fig. 2(a) verifies this finding graphically, according to which the two species, rather than outcompeting one another, are able to coexist at this asymptotically stable equilibrium point (shaded circle). The other three equilibrium points represented by open circles are unstable as no trajectory tends to $(0,0)$, $\left(\frac{K}{\beta}, 0\right)$ and $\left(0, \frac{K}{\beta}\right)$.

Fig. 2(b) illustrates the phase portrait of the system when $\beta < \alpha$. As analytically found earlier, the equilibria $\left(\frac{K}{\beta}, 0\right)$ and $\left(0, \frac{K}{\beta}\right)$ are both asymptotically stable (shaded circles). These equilibria divide the phase portrait into two regions, one containing initial points for which trajectories tend to $\left(\frac{K}{\beta}, 0\right)$, and the other containing initial points for which trajectories tend to $\left(0, \frac{K}{\beta}\right)$. In this case, coexistence of the two species is impossible, and one species will always win the competition for survival (i.e. competitive exclusion of one species by the other species). The winner of this competition is determined by the initial population sizes.

4.4. Previous work on Population Biology for Congestion Control

Previous work on congestion control involving mathematical models of population biology was proposed for the Internet on the basis of either improving the current TCP CC mechanism [14] or providing a new way of combating congestion [15]. The study of [14] couples the interaction of Internet entities that involved in CC mechanisms (routers, hosts) with the predator-prey interaction. This model exhibits fairness and acceptable throughput but slow adaptation to traffic demand. Recent work by [15] focuses on a new TCP CC mechanism based on the LV competition model which is applied to the congestion window updating mechanism of TCP. According to the authors, remarkable results in terms of stability, convergence speed, fairness and scalability are exhibited. However, these approaches are based on the end-to-end model of the Internet, which is completely different from the hop-by-hop nature of WSNs. **The novelty of our approach lies in the fact that the LV model is applied to WSNs in a hop-by-hop manner**.

5. The LV-based Congestion Control (LVCC) Approach

A WSN is considered to be analogous to an ecosystem. An ecosystem comprises of multiple species that live together and interact with each other as well as the non-living parts of their surroundings (i.e. resources) to meet their needs for survival and coexist. Similarly, a wireless sensor network involves a number of cooperative nodes. Each node has a buffer in order to store packets and is able to initiate a traffic flow. Traffic flows can be seen as species that compete with each other for available network resources while traversing a set of intermediate nodes forming a multi-hop path leading to the sink. The number of bytes per traffic flow corresponds to the population size of each traffic flow. In analogy with ecosystems, *the goal is expected to be the coexistence of flows*. In the rest of the paper, the terms flows and species are used interchangeably.

To investigate the decentralized and autonomic nature of the proposed approach, a network is divided into smaller neighborhoods called sub-ecosystems. Each sub-ecosystem involves all nodes that send traffic to a particular one-hop-away node (parent node). *The traffic flows initiated by each node play the role of competing species and the buffer (queue) capacity of the parent node can be seen as the limiting resource within the sub-ecosystem.* The number of bytes sent by a node within a given period refers to the population size of its flow. The population size of each flow is affected by interactions among competing flows as well as the available buffer capacities.

The proposed approach provides hop-by-hop rate adaptation by regulating the traffic flow rate at each node. *Each node is in charge of self-regulating and self-adapting the rate of its traffic flow i.e., the rate at which it generates or forwards packets. The traffic flows compete for available buffer capacity at their one-hop-away receiving node involved in the path leading to the sink*. Each sending node is expected to regulate its traffic flow rate in a way that limiting buffer capacities at all receiving nodes along the network path towards the sink are able to accommodate

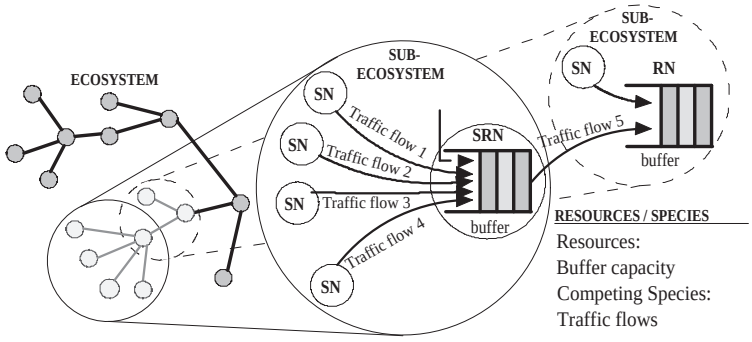

Figure 3: Traffic flows competition in WSNs.

all received packets. The sending rate evolution of each flow will be driven by variations in buffer occupancies of relay nodes along the network path towards the sink. Due to the decentralized nature of the proposed approach, thus satisfying the need for low communication overhead, each node will regulate its traffic flow rate using local information (i.e. from one-hop away neighbors).

Within a virtual ecosystem, participant nodes may perform different roles. In particular, each node is able to either initiate a traffic flow i.e. is a source node (SN), or serve as a relay node (RN) to forward packets of multiple flows passing through it, or perform both roles being a source-relay node (SRN). Source nodes are mostly located at the edges of a network (e.g. leaf nodes) while relay nodes are internal nodes (e.g. backbone nodes).

Pure **source nodes (SNs)** are end-entities which are attached to the rest of the network through a downstream node e.g., a relay node (RN), or a source-relay node (SRN) located closer to the sink. Each SN is expected to initiate a traffic flow when triggered by a specific event. The transmission rate evolution of each flow is calculated by Eq. 6 (the solution of Eq. 1) that gives the number of bytes sent x_i by flow i. In order to be able to solve Eq. 1 for a single node i, it is necessary to be aware of the aggregate number of bytes sent from all other nodes $\sum_{j=1,j\neq i}^{n} x_j$ which compete for the same resource. This quantity is denoted by C_i. In decentralized architectures, the underlying assumption of C_i-awareness is quite unrealistic. However, each SN can indirectly obtain this information through a small periodic backpressure signal sent from its downstream SRN/RN (parent node) containing the total number of bytes sent (BS) from all parent's children. Each node can evaluate its neighbors' contribution C_i by subtracting its own contribution x_i from the total contribution BS as expressed by: $C_i = \sum_{j=1,j\neq i}^{n} x_j = BS - x_i$. Thus, Eq. 1 becomes:

$$\frac{dx_i}{dt} = rx_i\left[1 - \frac{\beta}{K}x_i - \frac{\alpha}{K}C_i\right],\ i = 1, ..., n. \tag{6}$$

Eq. 6 is integrated to obtain the calculated transmission rate of each SN, x_i, given by:

$$x_i(t) = \frac{wx_i(0)}{\beta x_i(0) + \left[w - \beta x_i(0)\right]e^{-\frac{wr}{K}t}},\quad w = K - \alpha C_i. \tag{7}$$

A recent study by Antoniou et al. [16] focused on a network of n flows competing for a resource, where the populations of flows (number of bytes sent) are regulated by Eq. 7. It was found that such a network has a global non-negative and asymptotically stable equilibrium point

when inter-specific competition is weaker than intra-specific competition i.e., $\beta > \alpha$ and $\alpha, \beta > 0$. Recall that the same stability condition was analytically found for 2 species system (see Section 4). Under this condition, the other $n-1$ solutions of the n-species LV system are not stable. In the n-species LV system, the series of values generated by each SN when $\beta > \alpha$ converges to a global and asymptotically stable *coexistence solution* given by Eq. 8. For a detailed proof of this concept refer to [16].

$$x_i^* = \frac{K}{\alpha\,[n-1]+\beta},\ i = 1, ..., n. \tag{8}$$

Furthermore, in order to avoid buffer overflows, it needs to be ensured that when a system of n active nodes converges to the coexistence solution, each node i will be able to send less than or equal to K/n bytes. This is satisfied by Eq. 8 when $\alpha(n-1)+\beta \geq n$ or $\beta - \alpha \geq n \times (1-\alpha)$. If we set $\alpha \geq 1$ and require $\beta > \alpha$ (as imposed by the equilibrium stability condition), then the aforementioned inequality is always satisfied. Therefore, to ensure both convergence and no buffer overflows the following two conditions must be satisfied:

$$\beta > \alpha,\ \ \alpha > 1 \tag{9}$$

The calculated transmission rate of each node, $x_i(t)$, is initiated by $x_i(0)$ and converges to the stable coexistence solution, x_i^* within time T_{conv}. The convergence time, T_{conv}, can be evaluated by $x_i(T_{conv}) = x^*$ (on the basis of Eq. 7) and is found to be proportional to parameter α and inversely proportional to parameters r. This observation practically means that fast convergence can be achieved using small values of α or large values of r, but further discussion is given in performance evaluations.

Each SN adjusts its transmission rate on the basis of Eq. 7. This adjustment is carried out iteratively on a discrete-time basis, projecting the transmission rate from time t to some future time $t+T$ (i.e. over a time period T). For example, at the beginning of the $k+1$-th time period, $t = (k+1)T$, Eq. 7 is used to obtain the new transmission rate by the following calculation: set (a) $x_i(0)$ to the previous calculated transmission rate $x_i(kT)$, (b) t to the time duration T between the two successive transmission rate evaluations and (c) C_i to $C_i(kT)$ i.e. aggregate number of bytes sent from all competing nodes within the previous period. Therefore, Eq. 7 can be expressed in an iterative form as follows:

$$x_i((k+1)T) = \frac{w(kT)x_i(kT)}{\beta x_i(kT) + \left[w(kT) - \beta x_i(kT)\right] e^{-\frac{w(kT)r}{K}T}}. \tag{10}$$

Eq. 10 generates a series of values which correspond to number of bytes sent every period T.

Pure **relay nodes (RNs)** are entities which do not generate any packets, but forward packets belonging to several flows traversing themselves which compete for their resources. The main function of a RN is to combine (or multiplex) all incoming flows into a superflow and relay it to the dedicated downstream node (SRN or RN). Each RN allocates resources for its active upstream nodes based on a slightly modified expression of Eq. 10 as follows:

$$x_{RN}((k+1)T) = m\left[\frac{w(kT)H(kT)}{\beta H(kT) + \left[w(kT) - \beta H(kT)\right] e^{-\frac{w(kT)r}{K}T}}\right], \tag{11}$$

where $H(kT) = \frac{x_{RN}(kT)}{m}$, $w(kT) = K - \alpha C_{RN}^*(kT)$ and m is the total number of active upstream nodes which belong to the tree having RN as root. Each RN can calculate the number of its active

upstream nodes, m, by examining the source id field of each packet traversing itself. $C^*_{RN}(kT)$ reflects the total number of bytes sent (BS) to the downstream node from all its competing children nodes, subtracting the contribution of a single flow belonging to the superflow, given by:

$$C^*_{RN} = BS - \frac{x_{RN}(kT)}{m}. \tag{12}$$

A **source-relay node (SRN)** acts as both source and relay node, having both functions concurrently operated as described above.

6. Performance Evaluation

This section evaluates the performance of the LVCC approach and discusses its effectiveness in preventing congestion by mimicking the species competition. More specifically, realistic network simulations were conducted to show the basic features of the proposed bio-inspired mechanism such as *self-adaptiveness, scalability and fairness*. In addition, evaluation studies investigate how parameters affect the performance of our mechanism in terms of *stability and convergence* and provide effective parameter setting on the basis of congestion-oriented metrics.

Topology: The proposed mechanism was evaluated in a realistic network environment, using a series of representative network operation scenarios under NS2 networking simulator [17]. A WSN consisting of 25 wireless nodes was considered. The proposed approach can be efficiently and effectively used on top of routing or MAC protocols that create small depth (< 4) cluster/tree-based logical topologies over any physical topology. However, a detailed study of such protocols is beyond the scope of the current paper. In this paper, a dedicated routing protocol that creates the logical topology of Fig. 4 was assumed. The grey-shaded area represents a collision domain. For example, the nodes of cluster 1 (nodes 5, 6, 7, 8, and 9) will perceive each other's transmissions.

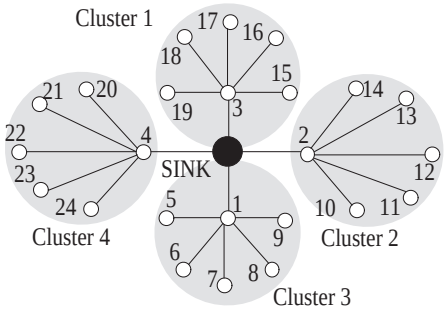

Figure 4: Evaluation cluster-based topology of 25 nodes (all links are wireless).

Test Parameters: The buffer capacity of each node was set to 35KB. The time period T between successive evaluations of the calculated rate of each SN, as well as the time between backpressure control packets was set to 1 sec. The selection of 1 second is guided by the desire to maintain responsiveness to changes in the network state and to avoid overwhelming the network with control packets. The CSMA-based IEEE 802.11 MAC protocol with 1Mbps transmission rate. Also, the two-ray ground radio propagation model was used.

Each node will transmit in one of 5 different levels namely, $1, 2, 4, 6$, and 8 Kbytes per $T = 1$ second (can be likened to video stored in multiple layers), starting from 1 Kbytes/T (i.e. 8 Kbps). Each node can increase its flow (or stream) rate to an upper level rate when the calculated transmission rate (obtained by Eq. 10) exceeds the specific upper level rate. Similarly, there should be a transition from the current level rate to a lower level rate when the calculated transmission rate falls below the current level rate but is above the lower level rate.

Performance measures: Two common performance measures for congestion control approaches were taken into account: the packet delivery ratio (PDR) and the end-to-end delay (EED). Packet delivery ratio is defined as the ratio of the total number of packets received by the sink to the total number of packets transmitted by source nodes. End to end delay is defined as the time taken for a packet to be transferred from a source node to the sink.

6.1. Preliminary analysis

Based on both buffer overflow avoidance and stability conditions, parameter α is lower bounded by 1 and upper bounded by β ($1 < \alpha < \beta$). However, analytical results show that low α and β values result in high calculated transmission rates at equilibrium, x^*, evaluated by Eq. 8. In addition, there is no upper limitation on β but as it becomes larger, the steady state traffic rate (Eq. 8) decreases. In this case, each active node will be limited to transmit data at a lower rate leading to lower quality of the received streams at the sink.

In order to supplement the analytical results, some theoretical model analysis scenarios were conducted using Matlab [18] in [19]. According to [19], Matlab experiments validated the correctness of analytical results, and showed that LVCC achieves graceful performance degradation, scalability, fairness and adaptability against changing traffic loads. In particular, this study showed that instability oscillations were observed at source nodes when the system was close to the stability limits ($\alpha \rightarrow \beta$). In addition, parameter α was found to be proportional to convergence time. Thus, fast convergence to the stable solution requires α to be close to 1 rather close to β (i.e. far from stability limits). On the other hand, low α values result in high calculated transmission rates at equilibrium that may not be accommodated by the underlying wireless medium. As far as the parameter β is concerned, a proper setting would be to choose the lowest value that ensures stability (i.e. not too close to α) and high calculated transmission rates at equilibrium (and thus, high quality), without causing wireless channel capacity saturation. Furthermore, it was shown that the value of r cannot grow unboundedly in order to achieve fast convergence. The value of r was tested across quite a large number of combinations of α and β values. Results showed that the calculated flow transmission rates were able to converge for every combination of α and β when $r \leq 2$. Parameter setting is further investigated in realistic network scenarios.

6.2. Parameter Setting and System Stability

In this section, the impact of parameters α, β and r on a realistic network environment is investigated. Each scenario, concerning different combinations of α, β and r values, was executed 10 times and the average values of metrics over all scenarios are presented below. The values of each parameter were chosen to be $4 \leq \beta \leq 7$, $1 \leq \alpha \leq 4$ (in order to satisfy the conditions of stability and buffer overflow avoidance), and $0.5 \leq r \leq 2$. Initially, parameter r was set to 1.

Fig. 5(a) illustrates the impact of α and β on packet delivery ratio (PDR) when 3 nodes were active. It can be observed that the mean PDR for all active nodes was close to 1 (i.e. the sink received almost all packets sent from all active nodes) for the majority of β and α values. More specifically, for high values of β as for example $6 \leq \beta \leq 7$, high PDR was achieved for almost all

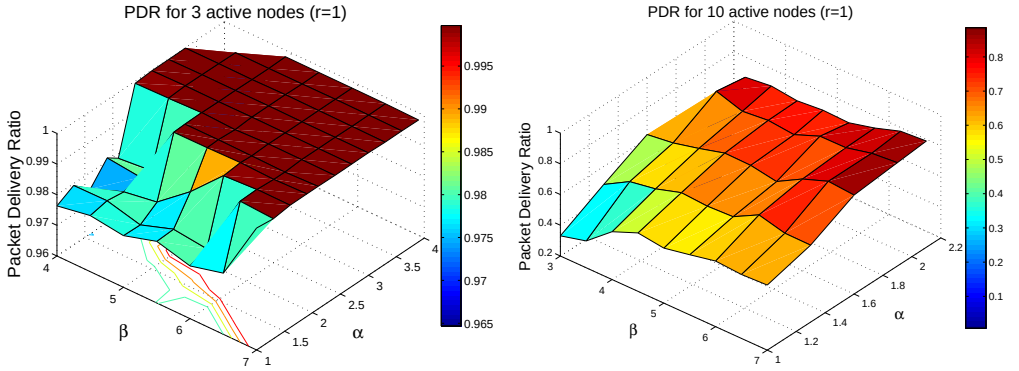

(a) 3 active nodes (b) 10 active nodes

Figure 5: Packet Delivery Ratio for 3 and 10 active nodes ($r = 1$).

values of α. Similarly, high PDR (close to 1) was achieved for lower β values $5 \leq \beta \leq 6$ when $2 \leq \alpha \leq 4$, and for $4 \leq \beta \leq 5$ when $2 \leq \alpha \leq 3$. Realistic network simulation results validated control system type simulations. In particular, the decrease in PDR perceived for low values of α was mainly attributed to the increase in calculated transmission rates at equilibrium. Thus, the increase of traffic load injection into the network provoked wireless channel contention leading to packet loss. In addition, a sharp decrease in PDR was observed when the stability condition was threatened, as for example for $3.5 \leq \alpha \leq 4$ and $\beta = 4$.

Fig. 5(b) presents the PDR for 10 active nodes. The highest PDR (≈ 0.9) was obtained for $6 \leq \beta \leq 7$ and $1.8 \leq \alpha \leq 2.1$. In addition, low delay values ($\approx 10\mu sec$) were achieved when α was set between 1.8 and 2.1, while β was ranging between 6 and 7.

Fig. 6 takes a closer look at the behavior of active flows under changing parameter values. The aim is to reveal how the violation of conditions for stability and buffer overflow avoidance could impact smooth network operation. In these scenarios, nodes $5, 6$ and 10 started transmitting at $t = 4, 74$ and 144 seconds respectively, while node 6 stopped transmitting at $t = 404$ seconds. Fig. 6(a) shows the calculated transmission rates of 3 active nodes for 3 combinations of parameter values. In these scenarios, the number of active flows changed over time (nodes 6 and 10 became active at $t = 74$ and $t = 144$ seconds respectively, while node 6 was deactivated at $t = 404$ seconds). As can be seen, when $\alpha = 1$ and $\beta = 0.8$, neither stability nor buffer overflow avoidance conditions were satisfied. Due to the violation of the first condition, only the flows of nodes 5 and 10 survived while the flow of node 6 became extinct. In addition, the calculated transmission rates of the survived active nodes exhibited cycle instability as shown in Fig. 6(a)(1). The phase plane of this scenario shown in Fig. 7 illustrates the oscillatory nature of the population of the two survived flows. Also, due to the violation of the second condition, the summation of calculated rates of the survived active nodes was greater than the buffer capacity of each node (35Kbytes), thus leading to buffer overflows.

As illustrated in Fig. 6(a)(2), when $\alpha = 0.25$ and $\beta = 0.5$, the stability condition was satisfied whereas the buffer overflow avoidance condition was violated. Fig. 6(a)(2) shows the calculated transmission rates after convergence, x^*, for each active node. As can be seen, the calculated transmission rate of each node is higher than or equal to 35 Kbytes/sec. However, nodes were

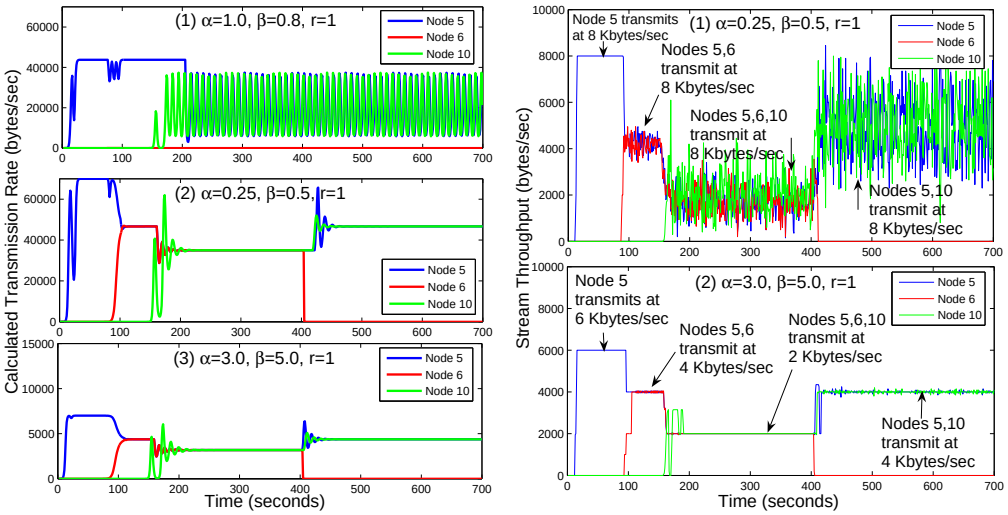

(a) Calculated transmission rates

(b) Stream throughput measured at the sink

Figure 6: Scenario with 3 active nodes ($r = 1$).

not transmitting at such high rates but at the highest predefined transmission rate of 8 Kbytes/sec throughout the scenario duration. Even though the buffer capacities within the network could accommodate the generated traffic load, collisions at the wireless channel led to packet loss. As a result, the stream throughput for each active node measured at the sink was fluctuating as shown in Fig. 6(b)(1). On the other hand, as shown in Fig. 6(a)(3), when $\beta = 5$ and $\alpha = 3$ none of the conditions were violated, while the calculated transmission rates were kept at lower values. Thus, each node was transmitting at the highest allowed predetermined transmission rate (see 6(b)(2)) without causing packet loss. Due to the low traffic load injected into the network in the presence of 3 active nodes, the mean end-to-end (EED) delay was kept below $4\mu sec$.

The results of Fig. 6(a) show that system stability can be preserved under dynamically changing traffic injection in the network caused by variation in the number of active nodes.

Analytical evaluations suggested that high values of r can contribute to fast convergence to the stable equilibrium solution. However, theoretical model analysis of complex scenarios in Matlab [19] showed that network stability was achieved for $r \leq 2$. Increasingly, realistic network experiments in NS2 showed that for $r < 1$, the calculated transmission rates of active nodes were not able to converge. Extensive NS2 simulation results showed that the value of r must be kept less than or equal to 2 in order to preserve system stability for all combinations of α and β values, regardless of the number of active nodes.

Further evaluation results showed that the mean PDR decreased slightly with the increase in the number of active nodes. The decrease of PDR was attributed to the inadequacy of network resources (e.g. wireless channel capacity) to accommodate the traffic load injected from a large number of active nodes. When the MAC transmission rate increased to 2 Mbps, higher PDR values were observed as a result of the enhanced channel capacity.

The values of parameters α, β and r should be chosen to ensure stability of traffic flows as well as buffer overflow avoidance. The parameter r can be set equal to 1 in order to preserve

convergence to equilibria as well as smooth flow rate regulation. However, the values of α and β depend on the number of active nodes, and thus could be adapted by each sending node according to the number of active nodes as follows:

$$\alpha = \begin{cases} 1.6, & 1 \leq n \leq 5; \\ 2.1, & 6 \leq n \leq 10. \end{cases} \tag{13}$$

$$\beta = \begin{cases} 4.3, & 1 \leq n \leq 5; \\ 7.0, & 6 \leq n \leq 10. \end{cases} \tag{14}$$

In a real WSN, the sink node is aware of the total number of active nodes within the network. The sink node can piggyback this number on control packets that are periodically broadcasted within the network. Each node can further spread this information out over the network by means of control packets.

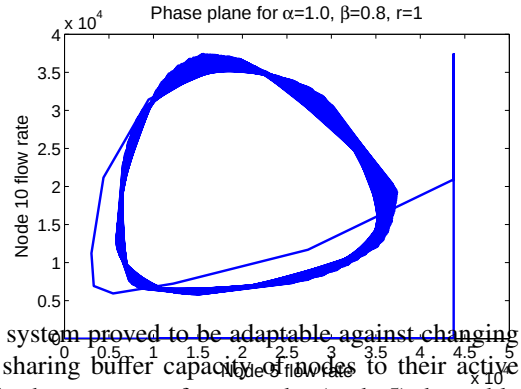

Figure 7: Phase plane for 5 bytes/T nodes.

6.3. Scalability and Fairness

Based on the results presented thus far, the system proved to be adaptable against changing traffic load and achieved scalability by fairly sharing buffer capacity of nodes to their active upstream nodes. For example in Fig. 6(a)(3), in the presence of one sender (node 5) the stable equilibrium point of the system given by Eq. 8 was 7000 bytes/T (clusterhead node 1 transmitted at the same rate). When node 6 became active, each sender obtained 4375 bytes/T, while the downstream node 1 was able to accommodate both senders by increasing its rate using Eq. 11. As the number of senders scaled up, all senders could be supported by the system by diminishing the sending rate per node, thus offering graceful degradation. Fairness was also achieved under changing conditions (nodes activation/deactivation), having the available buffer capacity of each node equally shared among all activated flows.

6.4. Comparative Evaluations

The proposed LVCC approach was compared with the traditional AIMD rate adaptation mechanism which is currently involved in recent congestion control protocols for WSNs [3], [6], [7]. The values of α, β and r were set to 2.4, 7 and 1 respectively, while scenarios 1 and 3 were considered, involving 3 and 5 active nodes respectively.

As shown in Figs. 8(a) and (b), the proposed LVCC approach achieved smooth throughput for each active node while maintaining friendliness among competing flows. This controlled behavior is attributed to the powerful LV-based calculated transmission rate evaluation which fairly shares the available network resources among active nodes.

On the other hand, as can be seen in Figs. 8(c) and (d), the AIMD approach displayed a saw-tooth behavior which represents the probe for available bandwidth. The oscillations shown in Figs. 8(c) and (d) were attributed to multiplicative rate decrease after packet loss events. Therefore, the AIMD rate control policy seems to be ineffective in wireless environments due to the frequent occurrence of packet loss events. In addition, AIMD seems inefficient for streaming applications since the saw-tooth rate behavior may violate the QoS requirements of a stream and can lead to significant variation in streaming media quality. Furthermore, the end-to-end nature of

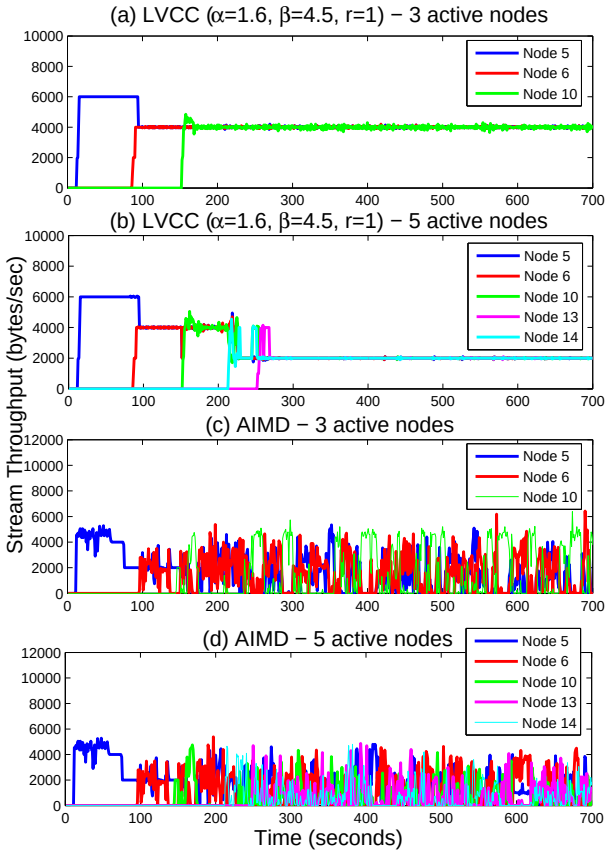

Figure 8: Throughput comparative evaluations between LVCC and AIMD for 3 and 5 active nodes.

the AIMD mechanism makes it incapable of operating in error-prone wireless multihop networks and results in reduced responsiveness, increased latency and high error rates, especially during long periods of congestion. Contrarily, the LVCC approach operates in a hop-by-hop manner, providing fast responsiveness to changing network conditions.

7. Conclusions and Future Work

In this paper, motivated by the famous LV competition model, a rate-based, hop-by-hop CC mechanism (LVCC) for small-scale multimedia WSNs was proposed. LVCC aims at controlling the traffic flow rate at each sending node. LVCC preserves the global properties of biological processes such as stability, self-adaptation, scalability and fairness, that are achieved collectively without explicitly programming them into individual nodes.

Realistic scenarios of network operation and conditions were performed to understand how the variations of the model's parameters influence stability, sensitivity to parameters, scalability and fairness. Performance evaluations suggested certain values for parameters α, β and r that are

able to achieve high packet delivery ratio, low end-to-end delay, scalability and fairness among competing flows. Furthermore, LVCC was found to outperform AIMD-like rate-based congestion control approaches for WSNs in terms of stability and flow rate smoothness. For future work, it is planned to investigate if and under what conditions parameter values can be analytically optimized using conventional or nature-inspired optimization techniques. In addition, the LVCC approach can be modified to cope with a set of different priority classes (e.g. by means of unequal traffic rates) corresponding to different kind of traffic flows.

Acknowledgment

This work is supported in part by the GINSENG: Performance Control in Wireless Sensor Networks project funded by the 7^{th} Framework Programme under Grant No. ICT-224282 and the MiND2C: Mimicking Nature for Designing Robust Congestion Control Mechanisms in Self-Organized Autonomous Decentralized Networks project funded by the Research Promotion Foundation of Cyprus under Grant No. TPE/EPIKOI/0308(BE)/03.

[1] I. Akyildiz, W. Su, Y. Sankarasubramaniam, E. Cayirci, Wireless sensor networks: a survey, Computer Networks 38 (2002) 393–422.

[2] I. Akyildiz, T. Melodia, K. R. Chowdhury, A Survey on Wireless Multimedia Sensor Networks, Computer Networks 51 (2007) 921–960.

[3] C. Wan, S. Eisenman, A. Campbell, CODA: Congestion Detection and Avoidance in Sensor Networks, Proc. of the 1st Int. Conf. on Embedded Net. Sensor Systems (2003) 266–279.

[4] B. Hull, K. Jamieson, H. Balakrishnan, Mitigating Congestion in Wireless Sensor Networks, Proc. of the 2nd Int. Conf. on Embedded Net. Sensor Systems (2004) 134–147.

[5] ICT FP7 GINSENG Project - Performance Control in Wireless Sensor Networks.
URL `http://www.ict-ginseng.eu/`

[6] S. Rangwala, R. Gummadi, R. Govindan, K. Psounis, Interference-Aware Fair Rate Control in Wireless Sensor Networks, Proc. of ACM SIGCOMM Symposium on Network Architectures and Protocols 36 (4) (2006) 63–74.

[7] L. Popa, C. Raiciu, I. Stoica, D. S. Rosenblum, Reducing Congestion Effects in Wireless Networks by Multipath Routing, Proc. of 14th IEEE International Conference on Network Protocols (2006) 96–105.

[8] K. Karenos, V. Kalogeraki, S. V. Krishnamurthy, Cluster-based Congestion Control for Sensor Networks, ACM Transactions on Sensor Networks 2008 4 (1).

[9] C. Y. Wan, S. B. Eisenman, A. T. Campbell, J. Crowcroft, Siphon: Overload traffic management using multi-radio virtual sinks in sensor networks, Proc. of ACM SenSys (2005) 116–129.

[10] F. Brauer, C. Chavez, Mathematical Models in Population Biology and Epidemiology, Springer, USA, 2000.

[11] A. Lotka, Elements of Physical Biology, Williams and Wilkins, Baltimore, MD, 1925.

[12] V. Volterra, Variations and fluctuations of the numbers of individuals in animal species living together, Animal Ecology (1931) 409–448.

[13] Phase portrait, (2009, october 25), In Wikipedia, the free encyclopedia. Retrieved May 5, 2010.
URL `http:en.wikipedia.orgwikiPhase_portrait`

[14] M. Analoui, S. Jamali, A conceptual framework for bio-inspired congestion control in communication networks, Proc. of the 1st BIMNICS (2006) 1–5.

[15] G. Hasegawa, M. Murata, TCP Symbiosis: Congestion Control Mechanism of TCP based on Lotka-Volterra Competition Model, Proc. of 2006 Workshop on Inter-perf 200.

[16] P. Antoniou, A. Pitsillides, Towards a Scalable and Self-adaptable Congestion Control Approach for Autonomous Decentralized Networks, 3rd European Symposium on Nature-inspired Smart Information Systems (NiSIS 2007).

[17] Ns-2 network simulator.
URL `http://www.isi.edu/nsnam/ns/`

[18] Matlab - the language of technical computing.
URL `http://www.mathworks.com/`

[19] P. Antoniou, A. Pitsillides, Congestion Control in Autonomous Decentralized Networks based on the Lotka-Volterra competition model, 19th International Conference on Artificial Neural Networks (ICANN 2009) 5769/2009 (2009) 986–996.